



## The effects of MEK and PKA inhibition on Spire proteins during oocyte maturation

Filiz Tepekoy<sup>1,2,3</sup>, Gokhan Akkoyunlu<sup>1\*</sup>

<sup>1</sup>Department of Histology and Embryology, Faculty of Medicine, Akdeniz University, 07070, Antalya, Turkey

<sup>2</sup>Center for Cell Dynamics, Department of Cell Biology, Johns Hopkins University School of Medicine, 855 North Wolfe Street, Baltimore, MD, 21205, USA

<sup>3</sup>Current Address: School of Human Sciences, College of Science and Engineering, University of Derby, Kedleston Road, Derby, DE22 1GB UK

### ARTICLE INFO

#### Original paper

#### Article history:

Received: February 15, 2023

Accepted: October 22, 2023

Published: December 10, 2023

#### Keywords:

Oocyte, mapk, mpf, spire-1, spire-2, actin

### ABSTRACT

Asymmetric division of oocytes driven by chromosome migration is a crucial step of oocyte maturation. Actin filaments take key roles in chromosome migration in oocytes. The aim of this study was to determine the effects of MEK and PKA inhibition on the levels of Spire-1 and Spire-2 proteins that are known to be related to actin nucleation. MEK inhibitor PD98059 and PKA inhibitor H89 were applied during IVM to the oocytes retrieved from preovulatory ovarian follicles of PMSG induced 3-5 weeks old female BalbC mice. GVBD and PBE rates were determined. Spire-1 and Spire-2 proteins were detected by immunofluorescence and western blot in oocytes at different maturation stages. Though GVBD rates were similar in different groups, PBE rates were lower in the MEK inhibition group. Through immunofluorescence, cortical localizations of Spire-1 and Spire-2 were determined. MEK inhibition resulted in a decrease in cortical Spire-1 and Spire-2 levels in PBE oocytes. PKA inhibition led to an increase in cortical Spire-1 levels in spindle migration stage oocytes, and an increase in cortical and total Spire-2 levels in PBE oocytes. Application of both MEK and PKA inhibition resulted in compensation of the decrease in Spire-1, while Spire-2 levels remained low with no compensation of PKA inhibition. According to the results of this study, chemical inhibition of MEK and PKA during oocyte maturation alters Spire-1 and Spire-2 protein levels.

Doi: <http://dx.doi.org/10.14715/cmb/2023.69.13.7>

Copyright: © 2023 by the C.M.B. Association. All rights reserved.

### Introduction

Oocyte maturation is a dynamic process in terms of molecular trafficking either activated or suppressed through the upstream regulators. The nuclear maturation of the oocyte covers the most prominent indicator of completion of meiosis I: germinal vesicle breakdown (GVBD) which is triggered by ovulation. Consequently, the oocyte enters the Meiosis II (MII) stage, which will be completed in case of activation by a spermatozoon (1).

The control of oocyte nuclear maturation is dependent on cyclic adenosine monophosphate (cAMP) levels in oocytes. Decreased levels of cAMP lead to the completion of meiosis and the progression of oocyte maturation (2, 3). High levels of cAMP in the oocyte suppress the activation of maturation promoting factor (MPF) through protein kinase A (PKA) which is a cAMP-dependent protein kinase (4, 5). MPF is a complex including catalytic cyclin-dependent kinase 1 ("cyclin-dependent kinase 1" =CDK1 or *Cdc2*) subunit and a regulator subunit cyclin B1(6). MPF activity is regulated by phosphorylation of highly conserved sites of *Cdc2*, which are Thr14 and Tyr15. The inhibitory phosphorylations at these sites are catalyzed by Wee1 kinases, and dephosphorylation of these sites is conducted by *Cdc25* phosphatases (7). PKA has been shown to directly affect the activities of both *Cdc25* phosphatases and Wee1 kinases (8). The mitogen-activated protein kinase (MAPK) signaling has been considered one of the principal regulatory cascades driving oocyte meiotic

progression and was shown to function in association with MPF (9).

The cytoplasmic maturation of the oocyte takes place synchronously with meiotic maturation. The cytoplasm of the oocyte matures through increasing numbers of the organelles and their alignment, generation of cortical granules, as well as the re-organization of the cytoskeletal components (10). This is a critical process in terms of both proper fertilization and early embryonic development (11).

The division of the oocyte is asymmetrical in terms of both the dimensions and developmental potential of the daughter cells (Sun and Kim, 2013). The oocyte can develop into an embryo whereas the polar body is degenerated. This asymmetrical division is necessary for a larger cytoplasm for the mature oocyte enabling sperm penetration, in addition to avoiding multiple fertilized oocytes under the same zona pellucida (12).

The germinal vesicle of oocyte arrested at prophase I, is centrally located. During in vitro maturation, while the chromosomes are aligned at the metaphase plate, the meiosis I spindle migrates to the cortex and initiates the anaphase. This process is called "chromosome migration" (13, 14). Extrusion of the polar body requires the movement and anchoring of the spindle towards the cortex and the driving force for this movement is the actin filament within the oocytes (15-17). Spire is one of the factors required for actin nucleation and polymerization (18) which includes 4 WH2 domains and monomeric actin-binding motifs required for actin nucleation (19). Spire has been shown

\* Corresponding author. Email: [gokhan\\_akkoyunlu@hotmail.com](mailto:gokhan_akkoyunlu@hotmail.com)

to play roles in the asymmetric division of mouse oocytes (20, 21).

Although it is known that, both Spire-1 and Spire-2 take part in the actin nucleation during the asymmetric division of the oocyte (20), the potential effects of inhibition of meiosis regulators on these proteins have not yet been investigated. In this study, we aimed to determine the effect of mitogen-activated protein kinase kinase (MEK) and PKA inhibition on Spire-1 and Spire-2 in mouse oocytes during *in vitro* maturation (IVM).

## Materials and Methods

### Oocyte collection and *in vitro* maturation

3-5 week Balb/C female mice were maintained under standard laboratory conditions ( $21 \pm 1$  °C; ambient temperature; controlled light/ dark conditions, 14L:10D) and were given food and water *ad libitum*. The experimental protocol was approved by the Institutional Animal Care and Use Committee at Johns Hopkins University. 5IU pregnant mare serum gonadotropin (PMSG) (Sigma Chemical Co., #G4527, St. Louis / MO, USA) was injected into the mice for follicle activation. After 48h of PMSG injection, the mice were sacrificed via cervical dislocation followed by CO<sub>2</sub> inhalation (22). 10 mice were used for each experiment. The ovaries from mice were placed in M2 medium (EMD Millipore, #MR-015-D, Billerica / MA, USA) including 0.2 mM 3-isobutyl-1-methylxanthine (IBMX) (Sigma Chemical Co., #I5879, St. Louis / MO, USA) priorly heated to 37°C following the dissection. GV oocytes were obtained from the antral follicles and isolated by an insulin injector under the stereomicroscope (Zeiss, Stemi SV-11-APO, Oberkochen / GERMANY). Hyaluronidase (Sigma Chemical Co., #H4272, St. Louis / MO, USA) was applied (5 min. 37°C, 5% CO<sub>2</sub>) to eliminate cumulus and granulosa cells. GV oocytes were collected by the mouth pipette and placed into M16 medium (*in vitro* maturation culture medium) (EMD Millipore, #MR-016-D, Billerica / MA, USA) with IBMX. Mineral oil (Sigma Chemical Co., #M5904, St. Louis / MO, USA) was used to avoid evaporation of 50 µL of medium droplets within the petri dishes. GV oocytes were cultured in 37°C, 5% CO<sub>2</sub> incubator for 3 hours within medium including IBMX. Consequently, the oocytes were transferred into M16 medium for culturing without IBMX for a particular time to obtain GVBD oocytes (2 hours), spindle formation (5 hours), spindle migration (7 hours), and polar body extrusion (PBE) (9 hours). During IVM, the oocytes were divided into four groups: 1) Control (dimethyl sulfoxide - DMSO) (Sigma Chemical Co., #276855, St. Louis / MO, USA), 2) MEK Inhibition (PD98059) (Cell Signaling Technology, #9900, Danvers / MA, USA), 3) MPF Activation (H89) (Cell Signaling Technology, #9844, Danvers / MA, USA), 4) MEK Inhibition (PD98059) + MPF Activation (H89). The experiments including these groups were replicated three times. The oocytes at particular stages of IVM were fixed for immunofluorescence or lysed for western blotting.

### MEK and PKA inhibition during IVM

To test whether Spire-1 and Spire-2 are associated with MAPK signaling, MEK protein was inhibited by specific chemical inhibitor PD98059 during IVM. 10µM, 25µM, and 50µM doses were applied during IVM for 2 hours (23).

To determine the efficiency of inhibition, total ERK1/2 and phosphorylated ERK1/2 levels which are dependent on MEK protein, were investigated through WB (Figure 1).

PKA was inhibited via chemical inhibitor H89 during IVM and the effect of this inhibition on actin nucleators Spire-1 and Spire-2 was detected. 0.1µM, 5µM, and 10µM doses were applied during IVM (24). The efficiency of the activator was tested through the cAMP response element-binding (CREB) protein which is a target for PKA. Total and phosphorylated CREB levels were determined by applying the WB (Figure 2).

### Immunofluorescence

The oocytes were fixed in 4% paraformaldehyde (PFA) (Affymetrix, #19943, Waltham / MA, USA) in phosphate-buffered saline (PBS) (Thermo Fisher Scientific, #10010023, Waltham/ MA, USA) and placed in microtubule stabilization buffer (25). The blocking was performed with 0.01 % Tween 20 + 2% BSA in PBS. The oocytes were incubated in Spire-1 (sc-85162) and Spire-2 (sc-136905) primary antibodies (1:100) at 4°C overnight. For each antibody, double staining with  $\alpha$ -tubulin (1:1000) (Sigma Chemical Co., T9026) was also performed. After wash steps with washing/blocking buffer, the secondary antibody incubation was performed for Spire-1(1:200) (AlexaFlour 488 anti-rabbit, ab150077), Spire-2 (1:200) (AlexaFlour 488 anti-goat, Thermo Fisher Scientific, A-11055) and  $\alpha$ -tubulin (1:200) (AlexaFlour 647 anti-rabbit (Thermo Fisher Scientific, A-20991) for 4 hours at room temperature. The oocytes were washed in washing/blocking buffer, stained with phalloidin (Thermo Fisher Scientific, #R415), and placed in a mounting medium with DAPI (Vector Labs, Burlingame, CA, USA, #H-1200). The stainings were observed under LSM-510 confocal microscope (Zeiss, Oberkochen, GERMANY). 3 different areas of 3 different oocytes were used for the analysis of each maturation stage.

### Western blot

The oocytes were lysed in Laemmli buffer with a protease inhibitor. The oocyte lysates were boiled for 5 min at 95 °C and left on ice, then separated on 10% polyacrylamide gels and transferred to a polyvinylidene difluoride (PVDF) membrane (26). 40 oocytes were placed in each well for detection of Spire-1, whereas 20 oocytes/well were used for Spire-2, p-ERK1/2 and p-CREB detection. Following the electrophoresis, proteins were transferred onto polyvinylidene fluoride (PVDF) membranes (Thermo Fisher Scientific, #88518, Waltham/ MA, USA) in a buffer containing 0.2 mol/l glycine, 25 mM Tris, and 20% methanol overnight. The successful transfer was confirmed by Ponceau S staining (Sigma Chemical Co., # P7170, St. Louis / MO, USA) of the blots. The membranes were blocked for 1 h with 5% bovine serum albumin (BSA) and 0.1% Tween 20 (Sigma Chemical Co., #P9416, St. Louis / MO, USA) in 0.14 mol/l Tris-buffered saline (TBS) (Thermo Fisher Scientific, #BP2471500, Waltham/ MA, USA) pH:7.2-7.4 at 4°C. Blotting membranes were incubated overnight at 4°C with ERK1/2 (1:1000) (Cell Signalling Technology (CST), #4695), p-ERK1/2 (1:1000) (CST-4370), CREB (1:1000) (CST-9197), p-CREB (1:1000) (CST-9198), Spire-1 (1:500) (Santa Cruz Biotech., sc-85162) and Spire-2

(1:500) (Santa Cruz Biotech., sc-136905) antibodies. After washing steps, the membranes were further incubated with secondary antibodies anti-rabbit HRP (1:2000) (CST-7074) for Spire-1, ERK1/2, p-ERK1/2, CREB, pCREB; anti-goat HRP (1:2000) (Thermo Fisher Scientific, #31402) for Spire-2 for 1 h at room temperature. Immunolabeling was visualized using the chemiluminescence-based Clarity Western ECL Substrate (Bio-Rad Laboratories, #1705060, Hercules / CA, USA), and the membranes were exposed to Hyperfilm (Thermo Fisher Scientific, #34089, Waltham/ MA, USA) via Medical Film Processor (Konica, #SRX101, Newark / NJ, USA).  $\beta$ -Tubulin antibody (CST-2146) was used as an internal control for each blotting. A representative experiment of the three performed was reported.

**Statistics**

The fluorescence intensity of Spire-1 and Spire-2 immunofluorescence labeling as well as the band intensity relative to  $\beta$ -Tubulin obtained from western blot experiments was determined by Image J (National Institutes of Health, Bethesda, MD, USA). p-ERK1/2 and p-CREB band intensities were normalized by total ERK1/2 and total CREB respectively. The data obtained from these analyses and GVBD and PBE rates were evaluated through Sigma Stat (Sigma Stat for Windows, version 3.0, Jandel Scientific Corp., San Rafael, CA, USA) via One-Way ANOVA tests. The data were represented as  $\pm$ SEM and statistical significance was determined as  $P < 0,05$ .

**Results**

**The effects of MEK and PKA inhibitors on p-ERK1/2 and p-CREB levels**

50 $\mu$ M of MEK inhibitor PD98059 significantly reduced p-ERK1/2 levels (Figure 1) When 10 $\mu$ M of PKA inhibitor H89 was applied, there was a significant decrease in p-CREB levels (Figure 2). These effective doses were chosen for MEK and PKA inhibition during IVM.

**Oocyte maturation rates**

GVBD and PBE rates in all experimental conditions during IVM were determined. Though the GVBD rate was similar for all groups, the PBE rate of the MEK inhibition group (PD98059) was significantly decreased (Table 1).

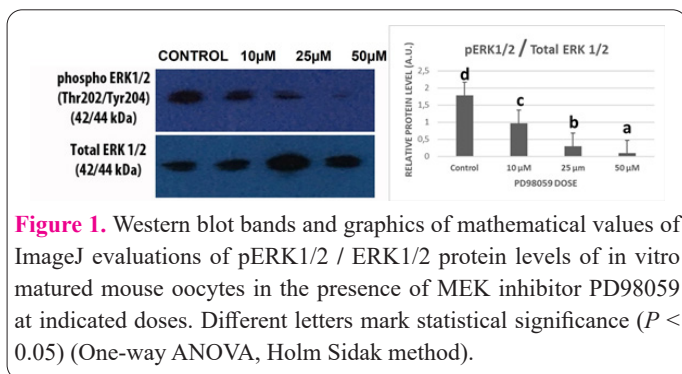


**Figure 1.** Western blot bands and graphics of mathematical values of ImageJ evaluations of pERK1/2 / ERK1/2 protein levels of in vitro matured mouse oocytes in the presence of MEK inhibitor PD98059 at indicated doses. Different letters mark statistical significance ( $P < 0.05$ ) (One-way ANOVA, Holm Sidak method).

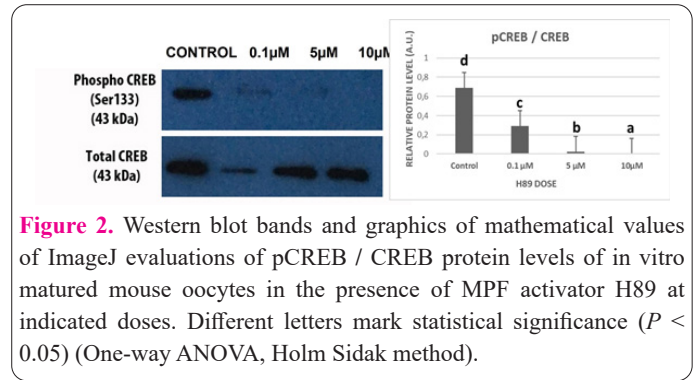


**Figure 2.** Western blot bands and graphics of mathematical values of ImageJ evaluations of pCREB / CREB protein levels of in vitro matured mouse oocytes in the presence of MPF activator H89 at indicated doses. Different letters mark statistical significance ( $P < 0.05$ ) (One-way ANOVA, Holm Sidak method).

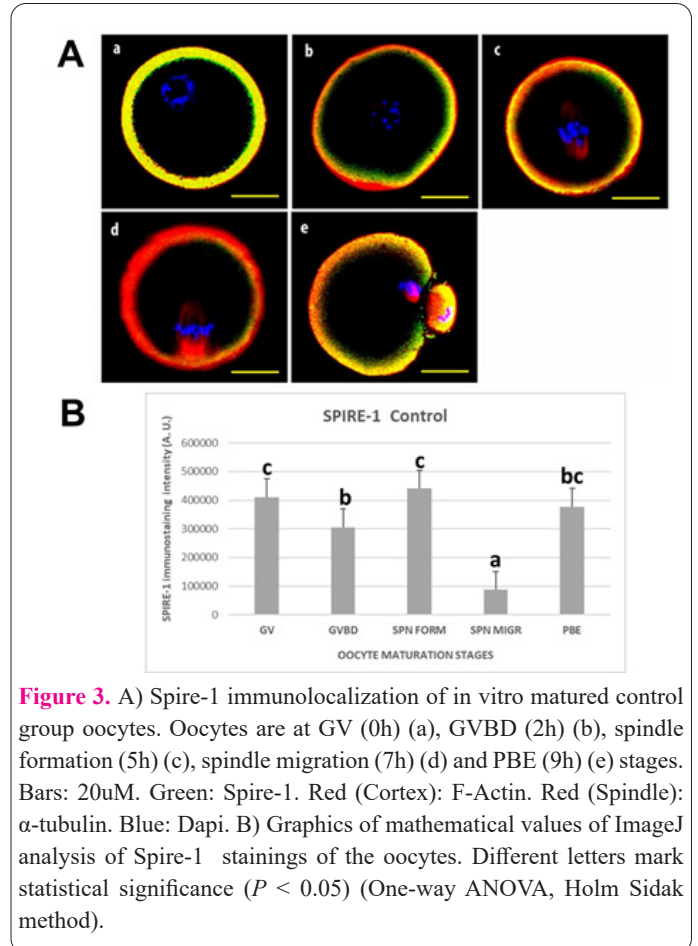


**Figure 3.** A) Spire-1 immunolocalization of in vitro matured control group oocytes. Oocytes are at GV (0h) (a), GVBD (2h) (b), spindle formation (5h) (c), spindle migration (7h) (d) and PBE (9h) (e) stages. Bars: 20 $\mu$ M. Green: Spire-1. Red (Cortex): F-Actin. Red (Spindle):  $\alpha$ -tubulin. Blue: Dapi. B) Graphics of mathematical values of ImageJ analysis of Spire-1 stainings of the oocytes. Different letters mark statistical significance ( $P < 0.05$ ) (One-way ANOVA, Holm Sidak method).

**The effect of MEK and PKA inhibition on Spire-1 levels in oocytes**

Cortical localization of Spire-1 was detected in oocytes by IF at all stages of meiotic maturation (Figure 3a). In the control group, higher staining density in the cortex of GV oocytes was detected. Cortical staining density was decreased in later stages, except for the spindle formation stage, and was significantly the lowest at the spindle migration stage (Figure 3b). WB results revealed that total protein level was similar in GV, GVBD, spindle formation, and PBE stages, but significantly decreased in the spindle migration stage (Figure 7).

In the presence of MEK inhibitor PD98059, Spire-1 cortical staining density was higher in GV oocytes (Figure

**Table 1.** Percentage of GVBD and PBE for different experimental conditions.

	CONTROL	PD98059	H89	PD9805+H89
GVBD	89.2 $\pm$ 2.3 <sup>a</sup>	85.6 $\pm$ 3.1 <sup>a</sup>	82.1 $\pm$ 2.5 <sup>a</sup>	84 $\pm$ 1.9 <sup>a</sup>
PBE	68.3 $\pm$ 1.4 <sup>b</sup>	52.2 $\pm$ 2.2 <sup>a</sup>	63 $\pm$ 2.9 <sup>b</sup>	59 $\pm$ 3.3 <sup>b</sup>

Among columns: a, b ( $P < 0.05$ ).

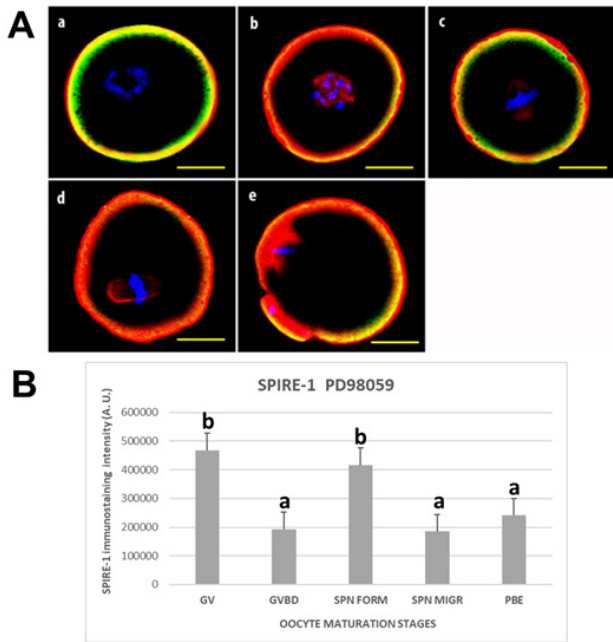


**Figure 4.** Spire-1 immunolocalization of in vitro matured PD98059 group oocytes. Oocytes are at GV (0h) (a), GVBD (2h) (b), spindle formation (5h) (c), spindle migration (7h) (d) and PBE (9h) (e) stages. Bars: 20uM. Green: Spire-1. Red (Cortex): F-Actin. Red (Spindle):  $\alpha$ -tubulin. Blue: Dapi. B) Graphics of mathematical values of ImageJ analysis of Spire-1 stainings of the oocytes. Different letters mark statistical significance ( $P < 0.05$ ) (One-way ANOVA, Holm Sidak method).

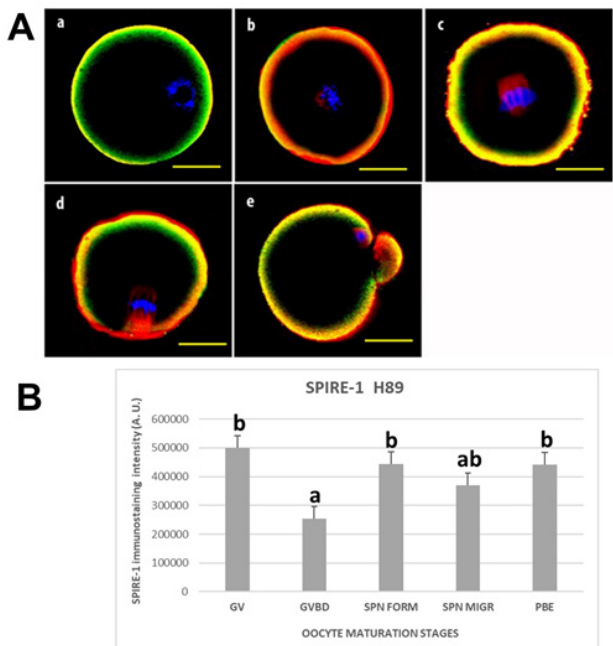


**Figure 5.** A) Spire-1 immunolocalization of in vitro matured H89 group oocytes. Oocytes are at GV (0h) (a), GVBD (2h) (b), spindle formation (5h) (c), spindle migration (7h) (d) and PBE (9h) (e) stages. Bars: 20uM. Green: Spire-1. Red (Cortex): F-Actin. Red (Spindle):  $\alpha$ -tubulin. Blue: Dapi. B) Graphics of mathematical values of ImageJ analysis of Spire-1 stainings of the oocytes. Different letters mark statistical significance ( $P < 0.05$ ) (One-way ANOVA, Holm Sidak method).

4a-b). WB results were also similar to the control group, showing that the protein level was significantly the lowest at the spindle migration stage (Figure 7).

When PKA was inhibited by H89, cortical staining was shown to be significantly decreased only at the GVBD stage. All the other stages showed similar levels of cortical localization (Figure 5a-b). According to WB results, the total amount of the protein was similar at all stages (Figure 7).

In the PD98059+H89 group, both cortical localization and the total level of the protein were shown to be significantly decreased at the GVBD stage by IF (Figure 6a-b) and WB (Figure 7).

### The effect of MEK and PKA inhibition on Spire-2 levels in oocytes

Through the IF, Spire-2 was also detected to be cortically localized in all experimental groups of oocytes. In the control group, Spire-2 staining density was the lowest in GV oocytes. It was shown to be increased at later stages, especially at spindle formation and PBE, while there was a significant decrease at the spindle migration stage (Figure 8a-b). Through the WB experiments, the total level of the protein was shown to be significantly increased after the GVBD stage and remained at higher levels until the PBE stage (Figure 12).

After MEK inhibition by PD98059, the staining density of Spire-2 was shown to be higher in the spindle formation stage. It was significantly lower in the PBE stage compared to the other stages (Figure 9a-b). According to the WB results, the total level of the protein was lower in GV and PBE stages (Figure 12).

PKA inhibition by H89 caused a slight decrease in the

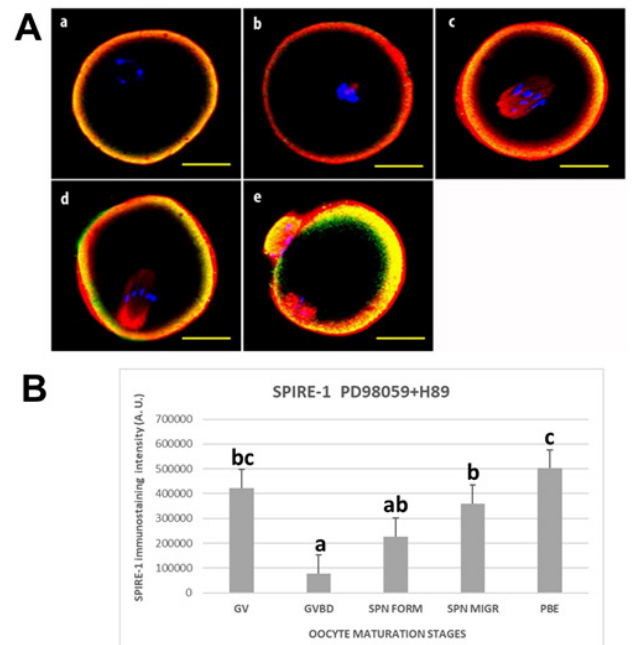


**Figure 6.** A) Spire-1 immunolocalization of in vitro matured PD98059+H89 group oocytes. Oocytes are at GV (0h) (a), GVBD (2h) (b), spindle formation (5h) (c), spindle migration (7h) (d) and PBE (9h) (e) stages. Bars: 20uM. Green: Spire-1. Red (Cortex): F-Actin. Red (Spindle):  $\alpha$ -tubulin. Blue: Dapi. B) Graphics of mathematical values of ImageJ analysis of Spire-1 stainings of the oocytes. Different letters mark statistical significance ( $P < 0.05$ ) (One-way ANOVA, Holm Sidak method).

4a-b). The oocytes at GVBD, spindle migration, and PBE stages showed a significantly lower staining density compared to GV and spindle formation stages (Figure

protein level was significantly the highest at the PBE stage and it was higher at the spindle migration stage compared to the other stages (Figure 12).

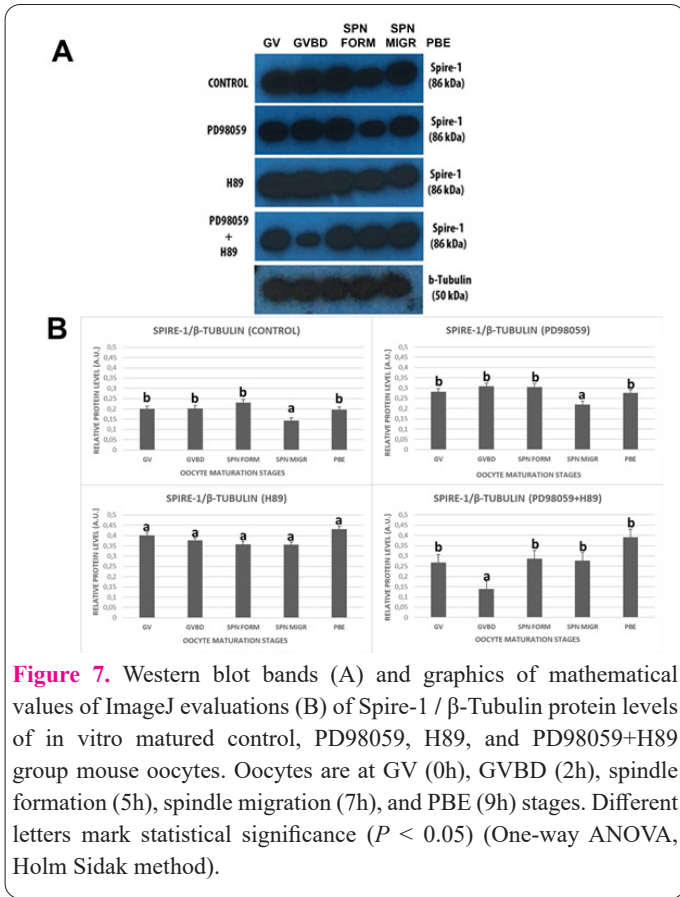


**Figure 7.** Western blot bands (A) and graphics of mathematical values of ImageJ evaluations (B) of Spire-1 /  $\beta$ -Tubulin protein levels of in vitro matured control, PD98059, H89, and PD98059+H89 group mouse oocytes. Oocytes are at GV (0h), GVBD (2h), spindle formation (5h), spindle migration (7h), and PBE (9h) stages. Different letters mark statistical significance ( $P < 0.05$ ) (One-way ANOVA, Holm Sidak method).

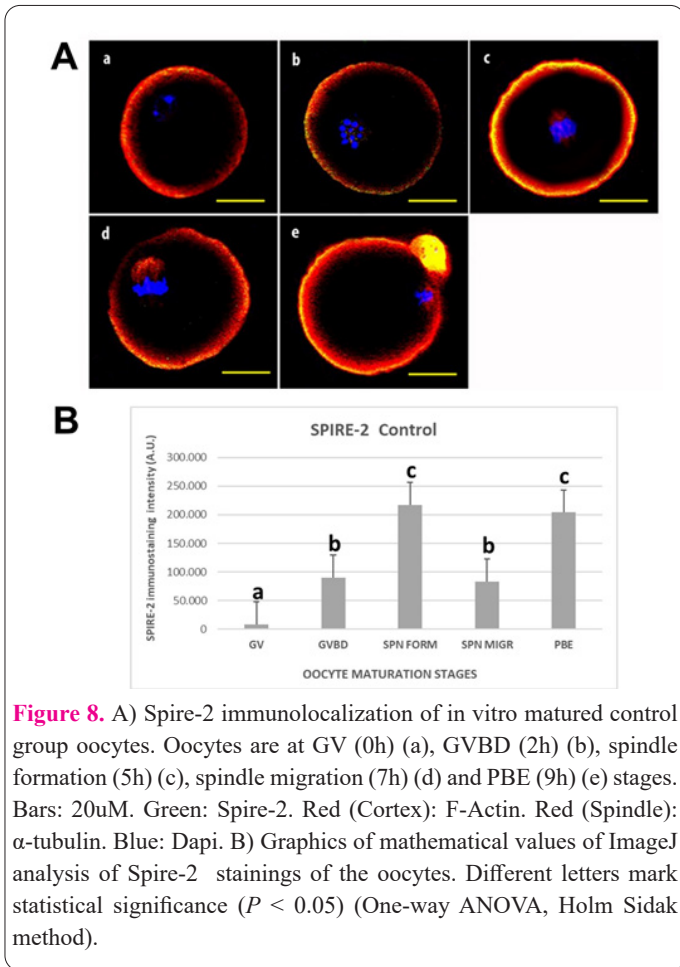


**Figure 8.** A) Spire-2 immunolocalization of in vitro matured control group oocytes. Oocytes are at GV (0h) (a), GVBD (2h) (b), spindle formation (5h) (c), spindle migration (7h) (d) and PBE (9h) (e) stages. Bars: 20uM. Green: Spire-2. Red (Cortex): F-Actin. Red (Spindle):  $\alpha$ -tubulin. Blue: Dapi. B) Graphics of mathematical values of ImageJ analysis of Spire-2 stainings of the oocytes. Different letters mark statistical significance ( $P < 0.05$ ) (One-way ANOVA, Holm Sidak method).

staining density of Spire-2 at GVBD and spindle formation stages. It was significantly lower in the spindle migration stage and was found to be the highest at PBE oocytes (Figure 10a-b). WB results also revealed that the total

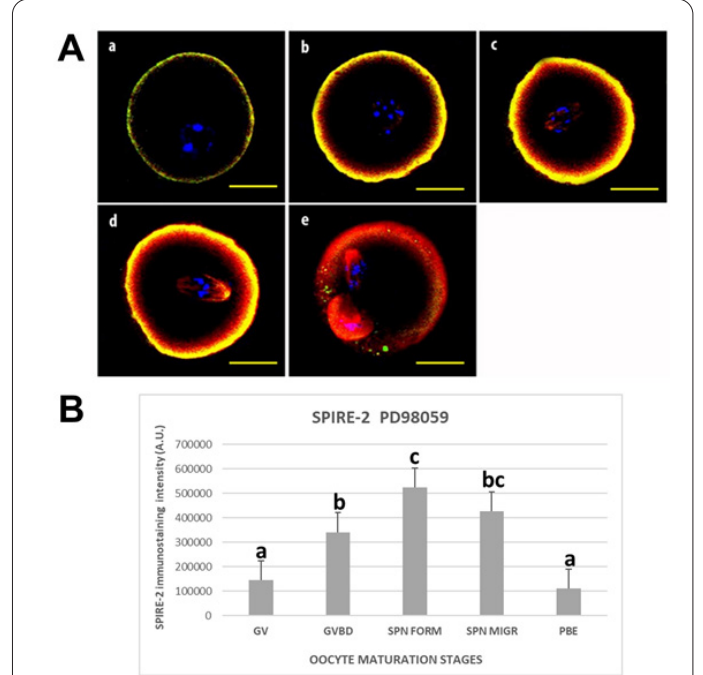


**Figure 9.** A) Spire-2 immunolocalization of in vitro matured PD98059 group oocytes. Oocytes are at GV (0h) (a), GVBD (2h) (b), spindle formation (5h) (c), spindle migration (7h) (d) and PBE (9h) (e) stages. Bars: 20uM. Green: Spire-2. Red (Cortex): F-Actin. Red (Spindle):  $\alpha$ -tubulin. Blue: Dapi. B) Graphics of mathematical values of ImageJ analysis of Spire-2 stainings of the oocytes. Different letters mark statistical significance ( $P < 0.05$ ) (One-way ANOVA, Holm Sidak method).

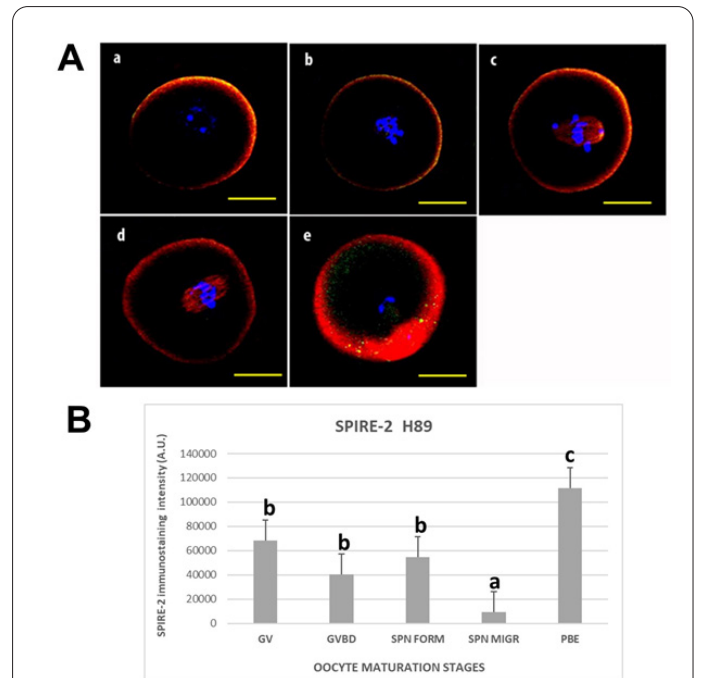


**Figure 10.** A) Spire-2 immunolocalization of in vitro matured H89 group oocytes. Oocytes are at GV (0h) (a), GVBD (2h) (b), spindle formation (5h) (c), spindle migration (7h) (d) and PBE (9h) (e) stages. Bars: 20uM. Green: Spire-2. Red (Cortex): F-Actin. Red (Spindle):  $\alpha$ -tubulin. Blue: Dapi. B) Graphics of mathematical values of ImageJ analysis of Spire-2 stainings of the oocytes. Different letters mark statistical significance ( $P < 0.05$ ) (One-way ANOVA, Holm Sidak method).

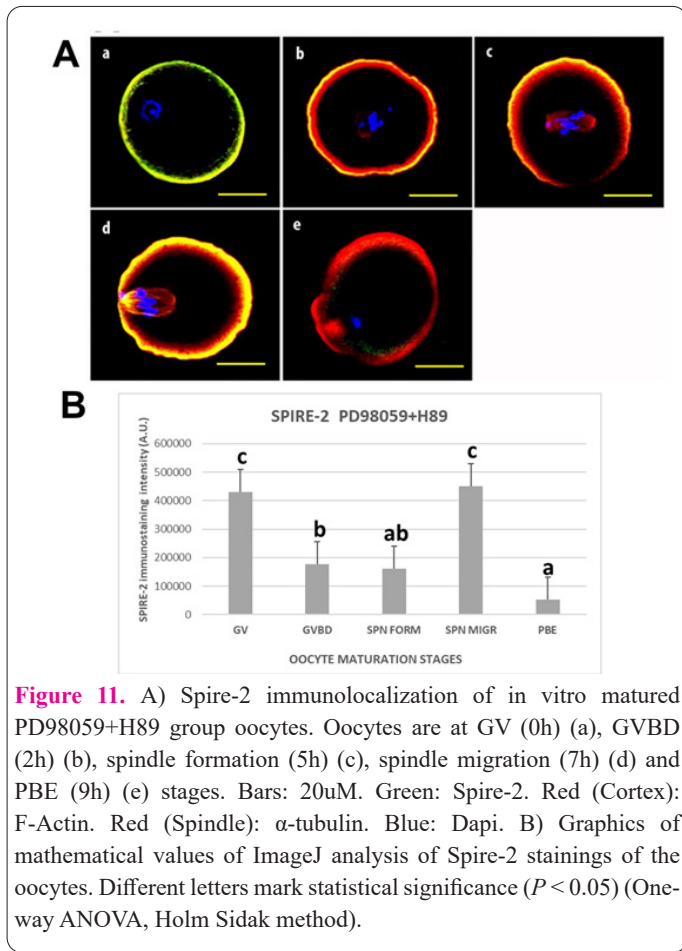


**Figure 11.** A) Spire-2 immunolocalization of in vitro matured PD98059+H89 group oocytes. Oocytes are at GV (0h) (a), GVBD (2h) (b), spindle formation (5h) (c), spindle migration (7h) (d) and PBE (9h) (e) stages. Bars: 20uM. Green: Spire-2. Red (Cortex): F-Actin. Red (Spindle):  $\alpha$ -tubulin. Blue: Dapi. B) Graphics of mathematical values of ImageJ analysis of Spire-2 stainings of the oocytes. Different letters mark statistical significance ( $P < 0.05$ ) (One-way ANOVA, Holm Sidak method).

In the PD98059+H89 group, the oocytes at GV and spindle migration stages had a significantly higher level of cortical Spire-2 according to the IF results. It was shown to be the lowest in the PBE oocytes (Figure 11a-b). WB results also revealed that the total protein level was significantly the lowest in PBE oocytes (Figure 12).

### Discussion

Actin nucleation in the oocytes is critical for a successful maturation process. Since the division plate of the cell is determined by the localization of the spindle, the migration of the meiotic spindle is a critical stage for the asymmetric cell division of mammalian gametes (15, 27). The chromosome migration and eventually asymmetric division of the oocytes are highly associated with the actin network and therefore actin nucleators have important roles in this process (28). Though it was revealed that actin is a driving force for asymmetric cell division in murine (29) and porcine oocytes (30), the mechanisms of actin remodeling required for the asymmetric division of oocytes remain unclear (28).

The presence of Spire-1 and Spire-2 has been determined in mouse oocytes (20, 31) and they were investigated in terms of their interaction with each other (20, 32). In this study, the potential effects of inhibition of meiotic regulators on these proteins were investigated.

In our study, Spire-1 density was shown to be higher in the cortex of oocytes during GV and spindle formation stages compared to the other stages through IF. Both IF and WB findings revealed that the level of Spire-1 was significantly decreased only at the spindle migration stage. These findings suggest that Spire-1 expression increases at

the early stages of oocyte maturation and after polar body extrusion. These results are compatible with the findings in the literature regarding actin dynamics at these stages (14).

MEK inhibition affected only cortical Spire-1 level in PBE stage oocytes which was shown to be significantly lower compared to the GV and spindle formation stages although it was similar in control group oocytes. Since Spire protein was shown to be related to PBE in previous studies (20), the decrease in the PBE levels of the oocytes in this study might be related to the decreased level of cortical Spire-1. PKA inhibition resulted in similar levels of Spire-1 at different maturation stages, whereas a decrease in the cortical localization at the GVBD stage was detected. Since PKA inhibition through H89 is expected to induce nuclear maturation (5), the findings in the current study suggest that activation of nuclear maturation factors might have elevated Spire-1 levels at most of the stages of oocyte maturation.

In the PD98059+H89 group, decreased level of Spire-1 was detected only at the GVBD stage. Thus, PKA inhibition through H89 might have compensated for the effect of MEK inhibition on Spire-1 levels at later stages of maturation.

In the current study, Spire-2 was also detected in the cortex of the oocyte through IF. Previous studies also revealed a high affinity of Spire-2 for negatively charged membranes (33). IF staining in our study demonstrated that cortical localization of Spire-2 was lower at GV, GVBD, and spindle migration stages compared to spindle formation and PBE stages. WB findings also revealed that the level of Spire-1 protein was lower at GV and GVBD stages. MEK inhibition through PD98059 resulted in a decrease in Spire-2 levels at the PBE stage. When PKA was inhibited, PBE stage oocytes showed higher

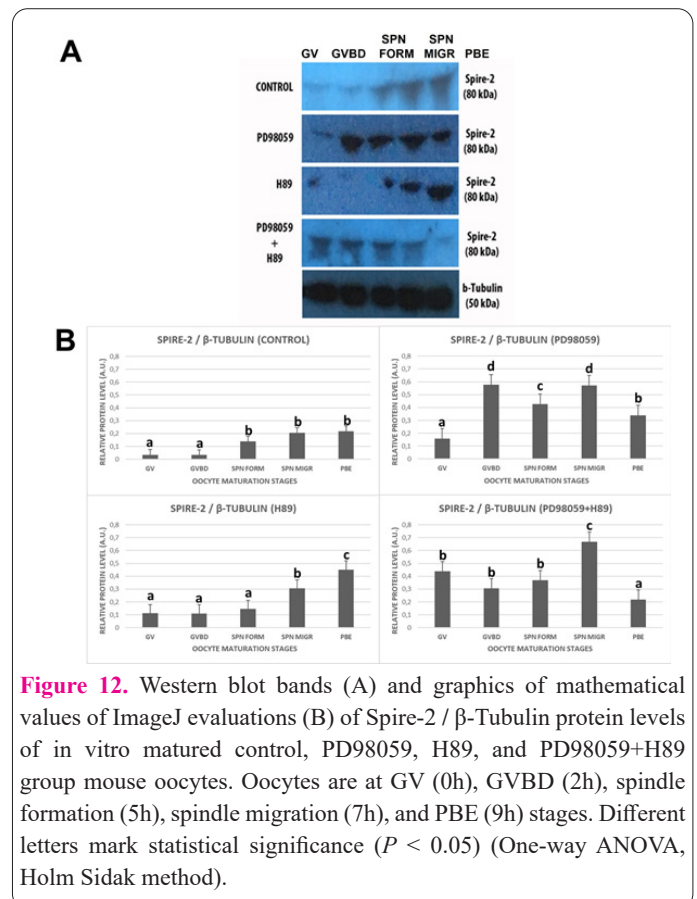


**Figure 12.** Western blot bands (A) and graphics of mathematical values of ImageJ evaluations (B) of Spire-2 /  $\beta$ -Tubulin protein levels of in vitro matured control, PD98059, H89, and PD98059+H89 group mouse oocytes. Oocytes are at GV (0h), GVBD (2h), spindle formation (5h), spindle migration (7h), and PBE (9h) stages. Different letters mark statistical significance ( $P < 0.05$ ) (One-way ANOVA, Holm Sidak method).

expression levels of the protein in this group both in IF and WB suggesting that PKA activation alters Spire-2 level at this particular stage. When both PD98059 and H89 were used, the Spire-2 level in PBE oocytes was decreased, suggesting that PKA inhibition could not compensate for the effect of MEK inhibition.

Mammalian oocytes contain two isoforms of MAPK: p44ERK1 and p42ERK2. Numerous studies have demonstrated the activation and involvement of these kinases during meiotic maturation (34). In our study, MAPK signaling was shown to be affecting Spire-1 and Spire-2 levels at particular maturation stages of oocytes. The factors affecting actin nucleation contribute to the correct positioning of the meiotic spindle during oocyte maturation (1, 35). These factors might be critical during fertility treatment when infertility is caused by abnormal maturation arrest of the oocytes. Although there are studies showing the association of different proteins with actin nucleation and actin-dependent spindle migration in oocytes (36-40), it remains unclear whether these proteins are driven by meiotic maturation factors.

Since Spire proteins are suggested to be important regulators of cytoplasmic maturation of oocytes (41), chemical manipulations related to Spire proteins during IVM could enhance the maturation levels and meiotic competence of the oocytes. The results of the current study demonstrate the effects of inhibition of MEK and PKA on Spire protein levels, suggesting that specific interventions during the IVM at the molecular level, would be essential for proper cytoplasmic maturation of oocytes.

### Acknowledgements

This work was supported by The Scientific and Technological Research Council of Turkey (TUBITAK) and by Akdeniz University, Scientific Research Projects Coordination Unit (2014.03.0122.006).

### Conflict of interest

The authors declare no conflicts of interest.

### Author contributions

F.T. and G.A. conceived the original idea. F.T. carried out the experiments. F.T. wrote the manuscript with support from G.A.

### References

- Li R, Albertini DF. The road to maturation: somatic cell interaction and self-organization of the mammalian oocyte. *Nat Rev Mol Cell Biol.* 2013;14(3):141-52.
- Conti M, Andersen CB, Richard F, Mehats C, Chun SY, Horner K, et al. Role of cyclic nucleotide signaling in oocyte maturation. *Mol Cell Endocrinol.* 2002;187(1-2):153-9.
- Wang X, Pepling ME. Regulation of Meiotic Prophase One in Mammalian Oocytes. *Front Cell Dev Biol.* 2021;9:667306.
- Bornslaeger EA, Mattei P, Schultz RM. Involvement of cAMP-dependent protein kinase and protein phosphorylation in regulation of mouse oocyte maturation. *Dev Biol.* 1986;114(2):453-62.
- Wang J, Cao WL, Liu XJ. Protein kinase A(PKA)-restrictive and PKA-permissive phases of oocyte maturation. *Cell Cycle.* 2006;5(2):213-7.
- Doree M, Hunt T. From Cdc2 to Cdk1: when did the cell cycle kinase join its cyclin partner? *J Cell Sci.* 2002;115(Pt 12):2461-4.
- Lew DJ, Kornbluth S. Regulatory roles of cyclin dependent kinase phosphorylation in cell cycle control. *Curr Opin Cell Biol.* 1996;8(6):795-804.
- Oh JS, Han SJ, Conti M. Wee1B, Myt1, and Cdc25 function in distinct compartments of the mouse oocyte to control meiotic resumption. *J Cell Biol.* 2010;188(2):199-207.
- Villa-Diaz LG, Miyano T. Activation of p38 MAPK during porcine oocyte maturation. *Biol Reprod.* 2004;71(2):691-6.
- Watson AJ. Oocyte cytoplasmic maturation: a key mediator of oocyte and embryo developmental competence. *J Anim Sci.* 2007;85(13 Suppl):E1-3.
- Conti M, Franciosi F. Acquisition of oocyte competence to develop as an embryo: integrated nuclear and cytoplasmic events. *Hum Reprod Update.* 2018;24(3):245-66.
- Otsuki J, Nagai Y, Lopata A, Chiba K, Yasmin L, Sankai T. Symmetrical division of mouse oocytes during meiotic maturation can lead to the development of twin embryos that amalgamate to form a chimeric hermaphrodite. *Hum Reprod.* 2012;27(2):380-7.
- Yi K, Rubinstein B, Li R. Symmetry breaking and polarity establishment during mouse oocyte maturation. *Philos Trans R Soc Lond B Biol Sci.* 2013;368(1629):20130002.
- Duan X, Sun SC. Actin cytoskeleton dynamics in mammalian oocyte meiosis. *Biol Reprod.* 2019;100(1):15-24.
- Verlhac MH, Lefebvre C, Guillaud P, Rassiner P, Maro B. Asymmetric division in mouse oocytes: with or without Mos. *Curr Biol.* 2000;10(20):1303-6.
- Yi K, Li R. Actin cytoskeleton in cell polarity and asymmetric division during mouse oocyte maturation. *Cytoskeleton (Hoboken).* 2012;69(10):727-37.
- Almonacid M, Terret ME, Verlhac MH. Actin-based spindle positioning: new insights from female gametes. *J Cell Sci.* 2014;127(Pt 3):477-83.
- Paunola E, Mattila PK, Lappalainen P. WH2 domain: a small, versatile adapter for actin monomers. *FEBS Lett.* 2002;513(1):92-7.
- Quinlan ME, Heuser JE, Kerkhoff E, Mullins RD. Drosophila Spire is an actin nucleation factor. *Nature.* 2005;433(7024):382-8.
- Pfender S, Kuznetsov V, Pleiser S, Kerkhoff E, Schuh M. Spire-type actin nucleators cooperate with Formin-2 to drive asymmetric oocyte division. *Curr Biol.* 2011;21(11):955-60.
- Vizcarra CL, Kreutz B, Rodal AA, Toms AV, Lu J, Zheng W, et al. Structure and function of the interacting domains of Spire and Fmn-family formins. *Proc Natl Acad Sci U S A.* 2011;108(29):11884-9.
- Leary S. AVMA Guidelines for the Euthanasia of Animals: 2013 Edition. American Veterinary Medical Association. . *Journal of the American Veterinary Medical Association.* 2013.
- Dudley DT, Pang L, Decker SJ, Bridges AJ, Saltiel AR. A synthetic inhibitor of the mitogen-activated protein kinase cascade. *Proc Natl Acad Sci U S A.* 1995;92(17):7686-9.
- Marunaka Y, Niisato N. H89, an inhibitor of protein kinase A (PKA), stimulates Na<sup>+</sup> transport by translocating an epithelial Na<sup>+</sup> channel (ENaC) in fetal rat alveolar type II epithelium. *Biochem Pharmacol.* 2003;66(6):1083-9.
- Messinger SM, Albertini DF. Centrosome and microtubule dynamics during meiotic progression in the mouse oocyte. *J Cell Sci.* 1991;100 ( Pt 2):289-98.
- Han SJ, Chen R, Paronetto MP, Conti M. Wee1B is an oocyte-specific kinase involved in the control of meiotic arrest in the mouse. *Curr Biol.* 2005;15(18):1670-6.
- Sun SC, Kim NH. Molecular mechanisms of asymmetric division in oocytes. *Microsc Microanal.* 2013;19(4):883-97.
- Namgoong S, Kim NH. Roles of actin binding proteins in mammalian oocyte maturation and beyond. *Cell Cycle.* 2016;15(14):1830-43.
- Longo FJ, Chen DY. Development of cortical polarity in mouse eggs: involvement of the meiotic apparatus. *Dev Biol.*

- 1985;107(2):382-94.
30. Kim NH, Day BN, Lee HT, Chung KS. Microfilament assembly and cortical granule distribution during maturation, parthenogenetic activation and fertilisation in the porcine oocyte. *Zygote*. 1996;4(2):145-9.
  31. Leader B, Lim H, Carabatsos MJ, Harrington A, Ecsedy J, Pellman D, et al. Formin-2, polyploidy, hypofertility and positioning of the meiotic spindle in mouse oocytes. *Nat Cell Biol*. 2002;4(12):921-8.
  32. Montaville P, Jegou A, Pernier J, Compper C, Guichard B, Mogessie B, et al. Spire and Formin 2 synergize and antagonize in regulating actin assembly in meiosis by a ping-pong mechanism. *PLoS Biol*. 2014;12(2):e1001795.
  33. Tittel J, Welz T, Czogalla A, Dietrich S, Samol-Wolf A, Schulte M, et al. Membrane targeting of the Spire-formin actin nucleator complex requires a sequential handshake of polar interactions. *J Biol Chem*. 2015;290(10):6428-44.
  34. Fan HY, Sun QY. Involvement of mitogen-activated protein kinase cascade during oocyte maturation and fertilization in mammals. *Biol Reprod*. 2004;70(3):535-47.
  35. Yi K, Unruh JR, Deng M, Slaughter BD, Rubinstein B, Li R. Dynamic maintenance of asymmetric meiotic spindle position through Arp2/3-complex-driven cytoplasmic streaming in mouse oocytes. *Nat Cell Biol*. 2011;13(10):1252-8.
  36. Pan ZN, Pan MH, Sun MH, Li XH, Zhang Y, Sun SC. RAB7 GTPase regulates actin dynamics for DRP1-mediated mitochondria function and spindle migration in mouse oocyte meiosis. *FASEB J*. 2020;34(7):9615-27.
  37. Pan ZN, Liu JC, Ju JQ, Wang Y, Sun SC. LRRK2 regulates actin assembly for spindle migration and mitochondrial function in mouse oocyte meiosis. *J Mol Cell Biol*. 2022;14(1).
  38. Hu LL, Pan MH, Yang FL, Zong ZA, Tang F, Pan ZN, et al. FASCIN regulates actin assembly for spindle movement and polar body extrusion in mouse oocyte meiosis. *J Cell Physiol*. 2021;236(11):7725-33.
  39. Jo YJ, Kwon J, Jin ZL, Namgoong S, Kwon T, Yoon SB, et al. WHAMM is essential for spindle formation and spindle actin polymerization in maturing mouse oocytes. *Cell Cycle*. 2021;20(2):225-35.
  40. Shan MM, Zou YJ, Pan ZN, Zhang HL, Xu Y, Ju JQ, et al. Kinesin motor KIFC1 is required for tubulin acetylation and actin-dependent spindle migration in mouse oocyte meiosis. *Development*. 2022;149(5).
  41. Jo YJ, Lee IW, Jung SM, Kwon J, Kim NH, Namgoong S. Spire localization via zinc finger-containing domain is crucial for the asymmetric division of mouse oocyte. *FASEB J*. 2019;33(3):4432-47.